Surface Kuroshio Intrusion Evidenced by Satellite Geostrophic Streamlines: Algorithm and Seasonal variations

Yisen Zhong[1], Meng Zhou[1], Joanna J. Waniek[2], Lei Zhou[1,3], Zhaoru Zhang[1]

[1]School of Oceanography, Shanghai Jiao Tong University, Shanghai, China, [2]Leibniz Institute for Baltic Sea Research Warnemünde, Seestraße 15, 18119 Rostock, Germany, [3]Southern Marine Science and Engineering Guangdong Laboratory (Zhuhai), Zhuhai, China.

Email: yisen.zhong@sjtu.edu.cn; meng.zhou@sjtu.edu.cn

Abstract

Using long-term satellite altimeter data, a new streamline-based algorithm is developed to identify the Kuroshio intrusion types and describe the seasonal variations of related dynamical properties. Results from this new classification show that a mixing of leaping, looping and leaking streamlines is the dominant form of Kuroshio intrusion into the South China Sea (SCS). The leaping path is very stable and crosses the Luzon Strait mainly through the Balintang Channel regardless of seasons, while the streamlines leaking into the SCS is more likely to intrude via the channel between the Babuyan Island and Camiguin Island. Large seasonal variations are found with the percentage of each kind of streamline and the Luzon Strait Transport (LST), but not with the intensity, width and current axis position of the Kuroshio. The along-streamline analysis reveals that the seasonal intrusion of the Kuroshio is essentially the seasonal variation of the cyclonic shear part of the flow. A possible physical mechanism is proposed to accommodate these seasonal characteristics based on globally the vorticity (torque work) balance between the basin-wide wind stress and the lateral friction, as well as locally the loss of balance between the torques of interior stresses and normal stresses both provided by the wall boundary, together with a plausible conjecture that the seasonally-reversing monsoon

can significantly modify the torque of the interior stresses within the cyclonic part of the flow and thus responsible for the seasonal variation of the Kuroshio intrusion.

Plain Language Summary

The Kuroshio Current, when flowing past the Luzon Strait, has a tendency of meandering into the Strait. The meandering current bifurcates with a branch into the South China Sea more frequently in winter than in summer. The reason why the Kuroshio intrusion varies seasonally remains unclear. In this study, a new streamline-based algorithm is developed, which facilitates us to investigate this problem with the long-term satellite data. We found that the Kuroshio width, intensity and position barely change within a seasonal cycle, and the intrusion branch is mainly the cyclonic shear part of the Kuroshio. The finding of these characteristics makes us look for a new interpretation for the seasonal intrusion. The global wind stress is responsible for Kuroshio leaping across the Strait, and the unbalanced torque of the lateral friction when the current loses contact with the wall tends to push the Kuroshio into the South China Sea. The strength of the unbalanced torque may be significantly modified by the seasonally-reversing monsoon. The combined effects explain the seasonal variability of the Kuroshio intrusion.

1. Introduction

The Kuroshio intrusion into the South China Sea (SCS) has been a long debate for decades (see the review paper by Nan et al., 2015). The warm and salty Kuroshio flows northwards along the eastern coast of Philippine. When encountering a boundary gap, Luzon Strait (LS) in this case, the current can either leap across the gap or bifurcates with a branch through the LS in the form of a loop current or a direct intrusion. The water enters the SCS mainly via the Balintang Channel and most of them subsequently exits through the Bashi Channel (Liang et al., 2008; Yuan et al., 2008). But the intrusion can efficiently exchange the momentum, heat and other tracers between the SCS and the Pacific (Nan et al., 2015; Qu et al., 2004; Wu, 2013;

Xu & Su, 2000).

To investigate the Kuroshio intrusion mechanism, the first step is usually to find a way to describe the Kuroshio intrusion paths and their variation in time. Previous methods almost always use the indirect parameters to indicate the variation of the intrusion such as an areal integral of geostrophic vorticity over the intrusion paths southwest of Taiwan (Nan et al., 2011a), the mean pressure (sea level anomaly) in a certain region west of the LS (Wu, 2013) etc. These parameters are indeed successful in interpreting many important findings on the intrusion characteristics on various time scales (Nan et al., 2015; Chen et al., 2020). However, the correlation between these parameters and the climate variables is usually not satisfactorily high, e.g. a correlation of 0.53 between Pacific Decadal Oscillation (PDO) index and interannual variability of intrusion shown in Wu (2013). The moderate correlation could be due to incompetent representation of intrusion with a single dynamical factor. Another issue with the traditional methods is that they typically categorize Kuroshio intrusion into three to five types using a subjectively determined threshold, but disregard the continual transition among different intrusion types. In other words, the variations of the strength of each intrusion type are not fully considered. This information may be essential for studying the intrusion mechanism especially when relating it to the variation of external forcing.

The Kuroshio intrusion has a strong seasonal cycle with more intrusion in winter and less in summer evidenced by both observational and modelling results. For decades a large volume of studies has been devoted to this topic (e.g. Farris & Wimbush, 1996; Hsin et al., 2012; Lan et al., 2004; Qu, 2000; Xu et al., 2004; Yang et al., 2013; Yaremchuk & Qu, 2004). However, the dynamical mechanism responsible for this remains unclear. The common knowledge is that the Kuroshio is nearly always bent into the LS but only a portion of the current can continue to move westwards into the SCS. The process of Kuroshio intrusion into the SCS can then be thought as a two-step problem. The first is what mechanism steers the Kuroshio into

the LS via different channels. Sheremet (2001) presents that the intrusion regime depends on the Reynolds number, i.e. the larger the transport or the inertia is, the more likely the flow leaps across the gap. He thus concludes that the Kuroshio normally leaps across the LS and penetrates into the SCS only when its strength is significantly reduced. The potential vorticity distribution is also found related to the intruding angle, speed and path (Nan et al. 2015; Sheu et al., 2010; Xue et al. 2004). Kuehl and Sheremet (2009) infer from the laboratory experiments that the Ekman transport may affect the Kuroshio intrusion by slightly changing the inflow angle.

The second problem can be stated as what drives the intrusion branch goes further into the SCS while not turns back to the path of the main stream, after the current enters the LS. On the seasonal time scale, this part of intrusion is primarily attributed to the local seasonally-reversing monsoon. Without the monsoon the upper Luzon Strait Transport (LST) could change from westward to eastward with misaligned seasonality (Hsin et al., 2012). Many previous studies show a close relationship between the intrusion transport and the wind-driven Ekman transport (Metzger & Hurlburt, 2001; Nan et al., 2001b), but the direct contribution of Ekman transport accounts for less than 10% of the total LST (Qu et al., 2004). Wu and Hsin (2012) show that the northwestward Ekman transport in winter can increase the probability of intrusion into the SCS by accelerating the upstream Kuroshio in the LS. They also point out that the existence of negative wind stress curl off the southwest Taiwan is crucial to triggering the intrusion.

The conclusions for the above two problems in previous studies come mainly from the laboratory or numerical experiments, owing to the lack of long-term in-situ measurements. Hence supports and validations from observational evidence are still needed. Currently only the satellite data can provide such a qualified tool to evaluate the variability of the surface, despite only geostrophic, transports of Kuroshio intrusion on various time scales. Song (2006) shows the (LST) is mainly geostrophic in the upper 1500 m, suggesting that the geostrophic transports derived from satellite

data are adequate to represent the major intrusion, given that the direct Ekman effect is proved to be small. In fact, various satellite products have been used to describe the intrusion patterns in a more qualitative manner (e.g. Farris & Wimbush, 1996; Yuan et al. 2006). In this study, we develop a new geometric method to both identify the intrusion types and quantify the seasonal variation of related dynamical properties using satellite altimetry data. A number of detailed but new findings are reported here and a suitable mechanism that accommodates these findings is then sought to interpret the seasonal variation of the Kuroshio intrusion.

2. Data and Method

2.1 **Satellite altimeter data**

The satellite data used here is the global ocean gridded L4 sea surface height from 1993 to 2018 reprocessed by Copernicus Climate Service. This product is suggested for studying ocean circulation and long-term variability because the processing focuses on the stability and homogeneity of the sea level records based on two-satellite constellation. Though multiple satellites can improve the spatial sampling, the introduction of a new satellite could lead to some biases and thus impair the data stability. The absolute dynamic height data is mapped onto a 0.25°×0.25° horizontal grid on a daily basis. As large biases may occur in the coastal region, the altimeter data in regions with water depth less than 300 m are discarded.

2.2 Streamline-based pattern recognition

Here we propose a geometric algorithm to recognize the flow pattern of Kuroshio intrusion into the SCS based on geostrophic streamlines derived from satellite altimeter data. For the surface geostrophic flow, the isopleth of sea surface level is a proxy of current streamline according to the geostrophic relation below.

$$u = -\frac{\partial \phi}{\partial y} = -\frac{g}{f}\frac{\partial \zeta}{\partial y}, \qquad v = \frac{\partial \phi}{\partial x} = \frac{g}{f}\frac{\partial \zeta}{\partial x}, \qquad \phi = \frac{g}{f}\zeta \#(1)$$

where ζ, u, v, ϕ are satellite sea surface elevation, longitudinal and latitudinal geostrophic velocities and geostrophic stream function respectively. By tracking the extension of streamlines originated from Kuroshio east of Philippine, different types of Kuroshio intrusion can be easily distinguished.

The Kuroshio Current, when encountering the LS, may bypass the Strait and go directly north, or take a detour to visit the SCS and then loop back to the main path, or intrude into the SCS directly. However, not all the time does the entire Kuroshio follow only one of the above routes. The current sometimes bifurcates with one branch going one way and the other going another. The 3L classification (Leap: bypassing, Loop: looping, Leak: bypassing and intruding, Nan et al. 2011a) describes three typical combinations of the above routes. Here we might as well borrow these three words to define the type for each Kuroshio streamline instead of the entire current. The Leap and Loop keep their original meanings while the Leak represents the streamlines that intrude the SCS. Each combination of these three kinds of streamlines makes one Current intrusion type, so in theory there should be seven types of current intrusion. As will be shown below, only four of them are important and the rest are either nonexistent or very rare (Table 1). The Kuroshio Current Loop could shed an eddy into the SCS from time to time. In this study we consider these eddies as a “gift” left by the loop current but not part of the main stream, therefore we will not categorize this type. Caruso et al. (2006) identifies a cyclonic loop intrusion type from the satellite sea surface temperature and the sea level anomaly, which cannot be distinguished by our algorithm as streamlines do not braid.

A series of criteria must be carefully defined to identify the above streamline types. We select the streamlines that pass through a transect along the latitude 19°N between 122°E and 124°E to represent the Kuroshio. This transect is located to the northeast of Philippine, where the entire incoming flow can be well captured. The west bound of the transect is located to the east of the Camiguin Island with water depth over 300 m, and the east bound is determined to make the transect slightly

longer than the width of the Kuroshio Current. This choice would not affect the final results because only the streamlines belonging to the above-mentioned types will be accounted in the subsequent analysis. The streamlines passing this transect with spatial interval of 0.01 m (isopleths of sea level) are tracked in the domain of 16–26°N and 110–126°E. Using equally-spaced isopleths renders the streamline number to represent the surface geostrophic transport. The Leap, Loop and Leak streamlines are defined according to the following criteria (Figure 1).

- If a streamline never intersects the 120°E longitude line but go north across the 22°N latitude line to the east of Taiwan, then it belongs to a Leap type.
- If a streamline intersects the 120°E line twice, which means going in and out of the SCS, then it belongs to a Loop type.
- If a streamline intersects the 120°E line only once, then it is a Leak one.

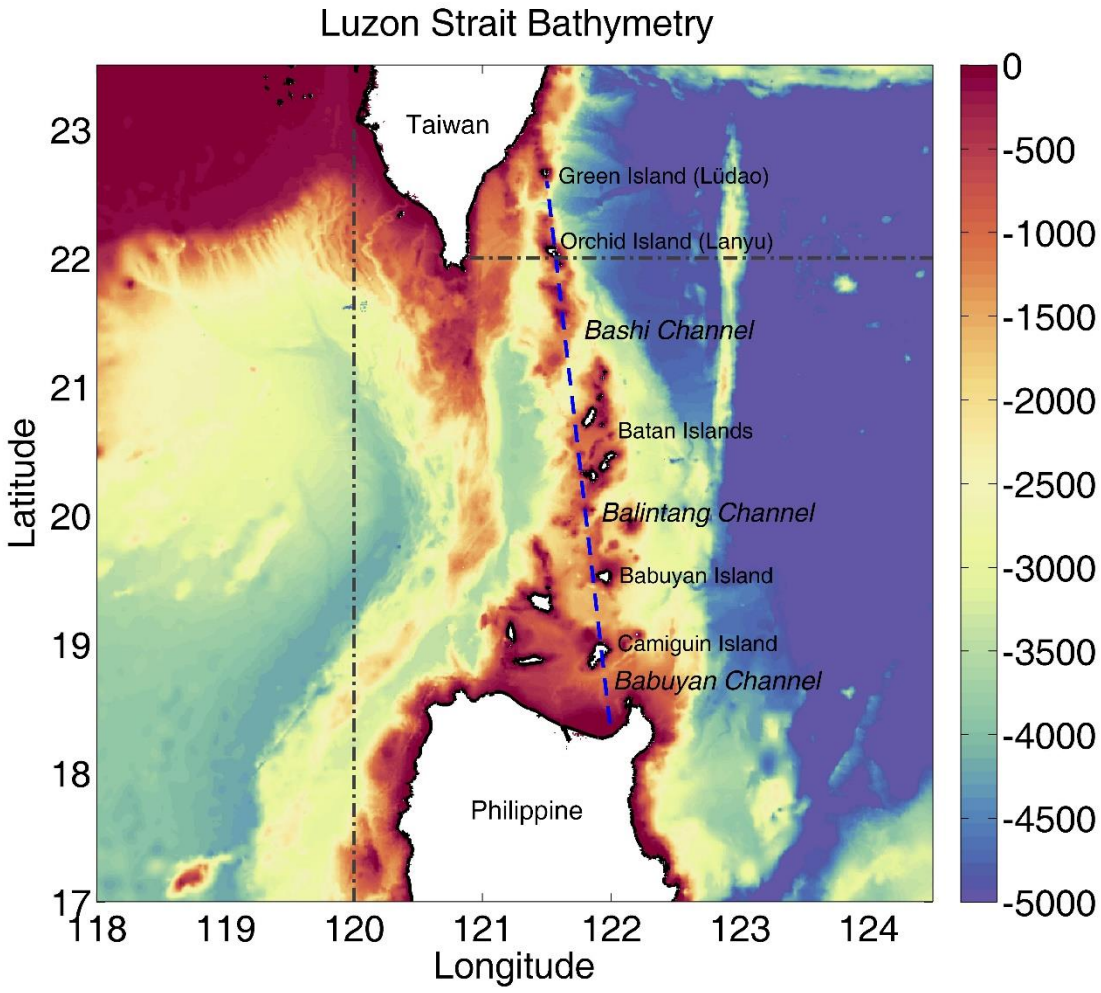

Figure 1: Bathymetry of Luzon Strait. The bathymetry data is from Shuttle Radar Topography Mission (SRTM). Two black dot-dash lines are along 120°E and 22°N and used to define streamline types. The blue dash line is defined as an approximate separatrix between the Luzon Strait and the Pacific used to judge whether the streamlines enter or exit the Strait.

The choice of 120°E longitude is somewhat subjective. A small shift will only make slight changes of the number of the Loop and Leap types, because there is no clear-cut definition for them by how far the Kuroshio meander reaches. Sometimes only a few streamlines on the outer edge of the flow loop across the 120°E line, while the majority of meanders still stay east of it. By tradition, we would probably call this a loop intrusion, even though the proportion of the loop is very small. In view of this, here we will not be concerned about the intrusion type of the entire Kuroshio but the statistics of the streamline intrusion types instead, e.g. what percentage of streamlines in the Kuroshio take a Leap/Loop/Leak path.

Our new algorithm inevitably has difficulty in identifying some streamlines which are apparently unrealistic in physics. For example, some Kuroshio streamlines may just end at the coast of Taiwan or Philippine inside the LS, possibly due to the coarse resolution of the dataset. Our results could also be inadequate to include all Kuroshio streamlines. For instance, there are some intrusion streamlines starting from the northern coast of Philippine. These streamlines might just be misrepresented by the coarse data but should be qualified for the true Kuroshio intrusion in reality. These issues will introduce some uncertainties in our calculation, but the excluded streamlines are expected to occupy only a small proportion and therefore have insignificant influence on the results.

3. Results

3.1 General statistics of Kuroshio intrusion

Four types of current intrusion are identified using our new method with typical examples demonstrated in Figure 2. Their occurrence frequencies calculated on a

daily basis are listed in Table 1. The leaping path accounts for nearly half of the days over the entire 26 years, about 10% higher than the probability presented in Nan et al. (2015). The second most probable scenario is a mixing of all three kinds of streamlines (Leap+Loop+Leak), which contributes nearly one fourth of the total (Fig.2d). This is a new current intrusion type detected using our method. It may be viewed as an intermediate phase between traditional loop and leak intrusion types (Leap+Loop and Leap+Leak streamlines). Interestingly, it turns out that this intermediate type occurs much more frequently than the Loop or Leak types, indicating that the looping and leaking paths are usually not separable, as opposed to that shown in previous classifications. The frequency of the pure loop intrusion is nearly twice as high as that of the leak intrusion, qualitatively in agreement with previous studies.

Different current intrusion types also show very strong seasonality (Table 1). The most prominent flow pattern in winter (taking December for an example) is the mixed intrusion type with a nearly half percentage, while in summer (June for example) the Leap type accounts overwhelmingly for more than 90% of the total cases. Note that no Leak type intrusion is detected in June by the algorithm. The Leak streamlines are all within the mixed current type. The rare occurrence of the Leak streamlines is indeed a unique feature of June as shown in the seasonal analysis below. The percentage of each kind of streamline in different current intrusion types is also presented in the Table 1 (inside the parenthesis). The Leap streamlines predominate at all times as expected. Notably it is actually the mixed type that contributes the largest proportion of the net intrusion transport into the SCS. During summer all types of intrusion are extremely weak.

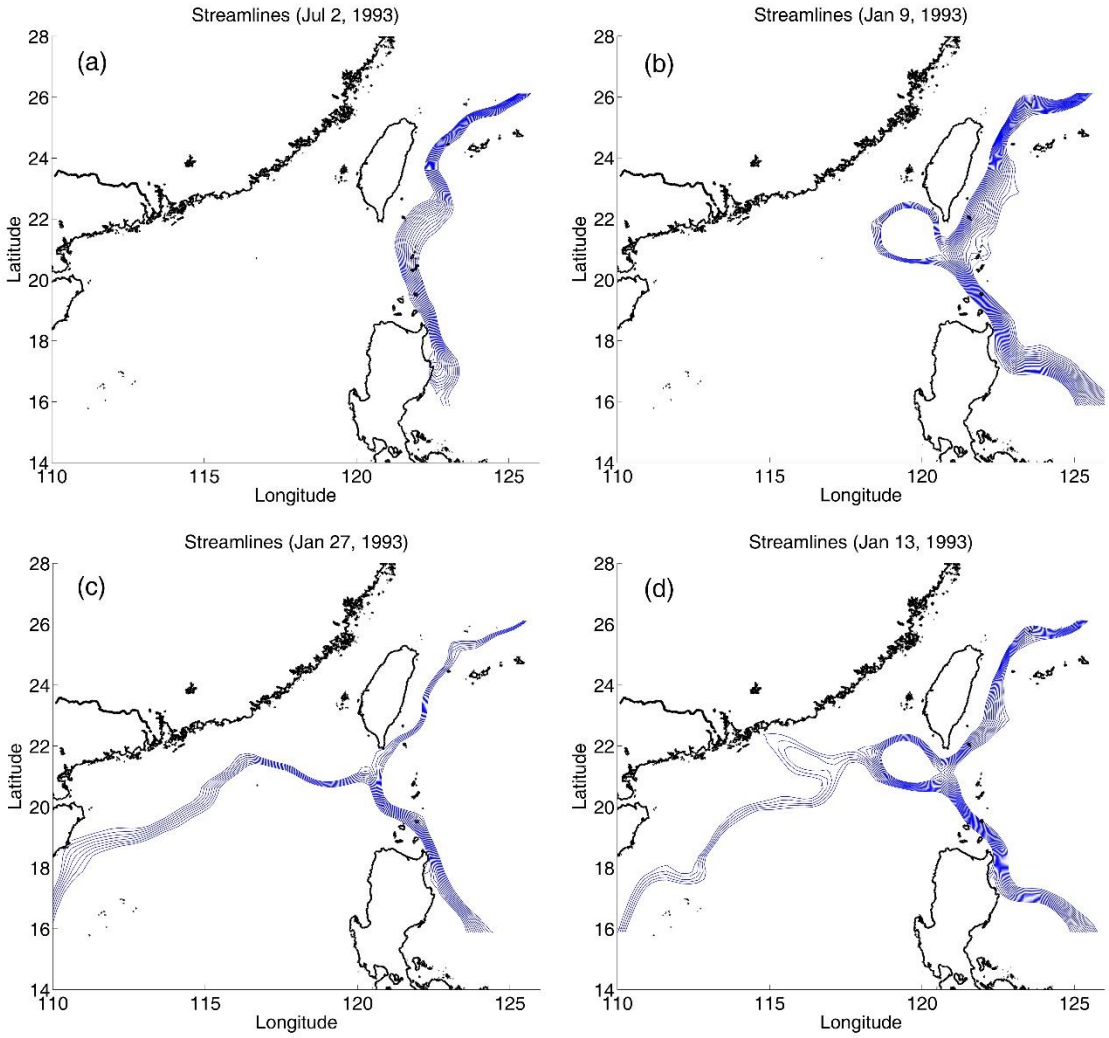

226

227 Figure 2: Examples of four Kuroshio Current intrusion types. (a) Leap; (b) Loop; (c) Leak; (d)

228 Mixed type.

Current intrusion type	**Streamline intrusion type**	**Frequency**	**Frequency in Dec**	**Frequency in Jun**
Leap	Leap only	49.0% (100%)	9.7% (100%)	91.7% (100%)
Loop	Leap+Loop	17.7% (76.2%+23.8%)	18.2% (57.1%+42.9%)	7.0% (80.7%+19.3%)
Leak	Leap+Leak	10.0% (68.6%+31.4%)	24.4% (61.6%+38.4%)	0% (N/A)
Mixed	Leap+Loop+Leak	23.3% (49.0%+25.2%+25.8%)	47.6% (42.7%+28.4%+28.9%)	1.3% (69.0%+14.0%+17.0%)

229 Table 1: Current intrusion types, Streamline intrusion types and their frequencies over the entire

230 period, in winter and summer respectively. In all frequency columns, the percentage in the

parenthesis indicates the percent of each streamline type in the respective current intrusion types.

A certain amount of the Kuroshio streamlines meanders into the LS all the time, no matter what current intrusion type it is (Figure 2). The traditional viewpoint is that the Kuroshio enters the LS mainly through the Balintang Channel and exit the Strait via the Bashi Channel (e.g. Liang et al., 2003, 2008; Yuan et al., 2008a). Here we define the boundary between the LS and the western Pacific by drawing a straight line roughly along the island chain from the Green Island to the Camiguin Island (blue dash line in Figure 1). With this definition, about 80% of the streamlines intrude into the LS over the entire period. Figure 3 shows that the latitudinal distribution of the entrance for each kind of streamline over the whole period, since it is not quite seasonally dependent. Most of the Leak streamlines intrude into the Strait through the channel between the Babuyan Island and the Camiguin Island (between 19°N and 19.5°N), while the Balintang Channel (between 19.5°N and 20.5°N) is the passage most Leap streamlines take. The distribution of the Loop streamlines more or less lies in between. As for the exit latitudes, both of the Loop and Leap streamlines tend to get out of the Strait between 21.5°N and 22.5°N, i.e. the upper half of the Bashi Channel and the channel between the Green Island and the Orchid Island, and the latter seems to have a slightly larger proportion (Fig.3d, e).

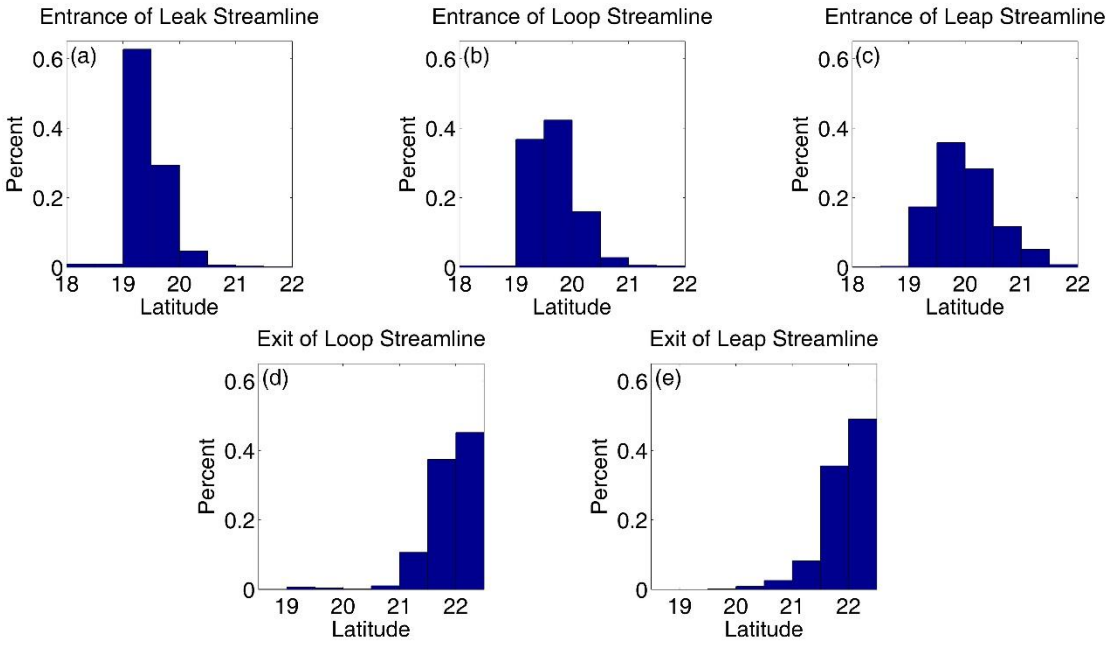

Figure 3: The entrance and exit latitudes of each type of streamlines over the entire period.

Figure 4 calculates the daily-averaged number of different streamlines binned onto a 0.25°×0.25° grid in June and December. Given that the loop intrusion can be seen as an intermediate state between the penetrating and the leaping regime, in the subsequent discussion we will focus on the Leak and Leap streamlines only in June and December, the months with the maximum leaping and the maximum intrusion respectively in a seasonal cycle. The path of the Leap streamlines looks quite stable and independent of any external seasonal forcing (Fig 4c, d). The winter Leak streamlines can generally extend further westwards and their routes are subjected to a large variance once the streamlines are out of the Strait. In summer, the very small number of intrusion streamlines tends to move northwards and end up at the coast. In spite of this unrealistic ending, the direction of the flow could be plausible, possibly due to the steering effect by seasonally-reversing monsoon.

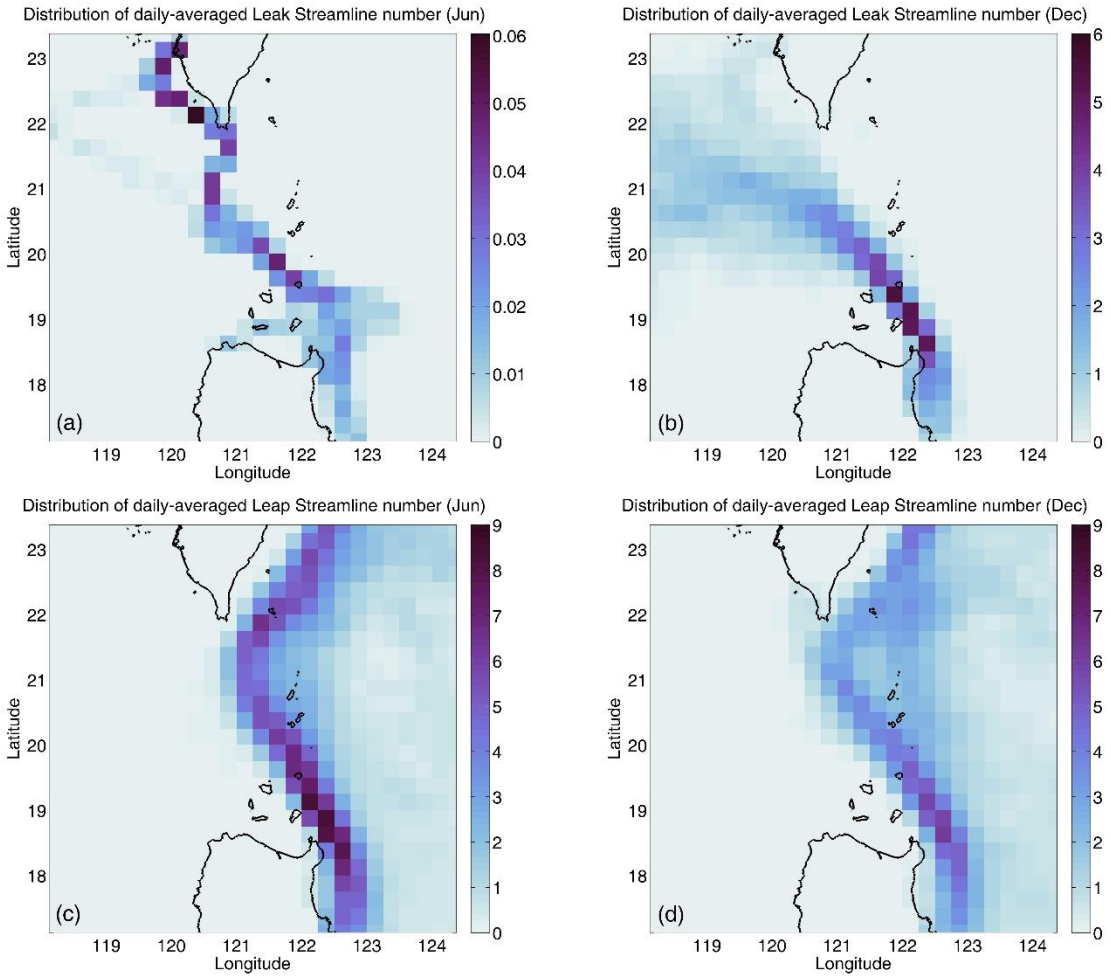

Figure 4: The average streamline number binned onto a 0.25×0.25 grid. Note the large difference in color range.

3.2 Seasonal variation of Kuroshio intrusion

The characteristics of the seasonal variation of Kuroshio intrusion have been well documented in a large volume of studies from both observational data and numerical modeling results. Unlike the general classifications of the flow pattern in previous works, the results presented here provide a different measure from streamline perspective. Figure 5 shows the seasonal percentages of each type of streamline. The advantage of this statistics is that it can more accurately reflect both the amount and the variation of different flow behaviors. The dominant Leap type varies between around 60% in winter and over 95% in summer. The Leak streamline reaches the maximum over 20% in December and reduces to a negligible value in

June. Though there is a large probability of intrusion in winter (Nan et al., 2015), the actual Leak streamlines only account for a small portion of the total Kuroshio. The Loop intrusion has nearly the same proportion as the Leak in winter and retains only a small amount in summer. In addition, not all of the streamlines that leak into the SCS will flow westwards and impact the slope current of the northern SCS. The percentage of the along-slope intrusion streamlines has a similar variation on both seasonal and interannual scales (not shown). In terms of the intrusion into the LS as defined in Section 3.1, the seasonal variability is the same but weaker, with the intrusion percentage ranging between 16% in winter and 24% in summer.

The surface geostrophic transport is calculated by accumulating the value differences of adjacent stream functions from Equation (1). The magnitude of the mean surface transport is roughly the same as that given in Qu et al. (2004), but subject to large standard deviations particularly in winter. According to Song (2006), the westward LST above 1500 m can be estimated by the geostrophic flow. Here assuming an upper 1500 m transport with the vertical distribution having an e-folding depth scale of 500 m, the estimated total transport is approximately varying from 0.03 to 5.0 Sv seasonally. These very rough estimates are in a reasonable range referring to the in-situ measurements and numerical outputs (Table 1 in Nan et al., 2015). Many studies suggest that during some months of a year the net LST reverses from the SCS to the Pacific (Xue et al., 2004; Yang et al., 2010). Since we only track the Kuroshio streamlines, the results here only account for the westward intrusion from Kuroshio, not the total LST.

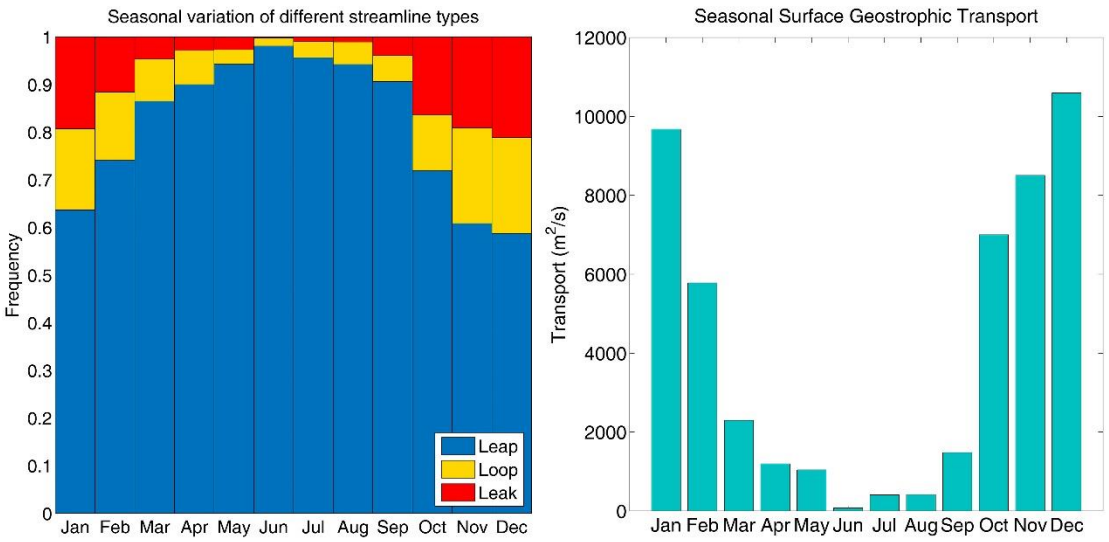

298

299 Figure 5: Seasonal variation of the occurrence frequency for the three types of streamlines over
300 the entire period (left); Seasonal surface intrusion geostrophic transport estimated based on the
301 Leak streamline number (Right).

302 The seasonality of the Kuroshio Current axis position is also examined along
303 18°N by two different methods. The first one is based on the maximum density of
304 streamlines, i.e. maximum velocity, and the other uses the longitude where the
305 zero-vorticity line is located. Both methods estimate the current axis around 50 km
306 away from the coast with nearly invisible seasonal difference (~ 5 km). Figure 6
307 shows the seasonal kinetic energy distribution in June and December. The width and
308 intensity of Kuroshio before turning round into the Strait make slight difference
309 between the months, and so does the surface transport (Chang & Oey, 2011). The
310 geostrophic flow is accelerated at the turning corner probably because a larger
311 pressure gradient is needed to offset the extra centrifugal force. In winter the Kuroshio
312 has more intrusion streamlines, so the curvature is slightly larger, while in summer the
313 streamlines primarily belong to the Leap type, leading to a weaker acceleration
314 associated with the smaller curvature (Fig.3).

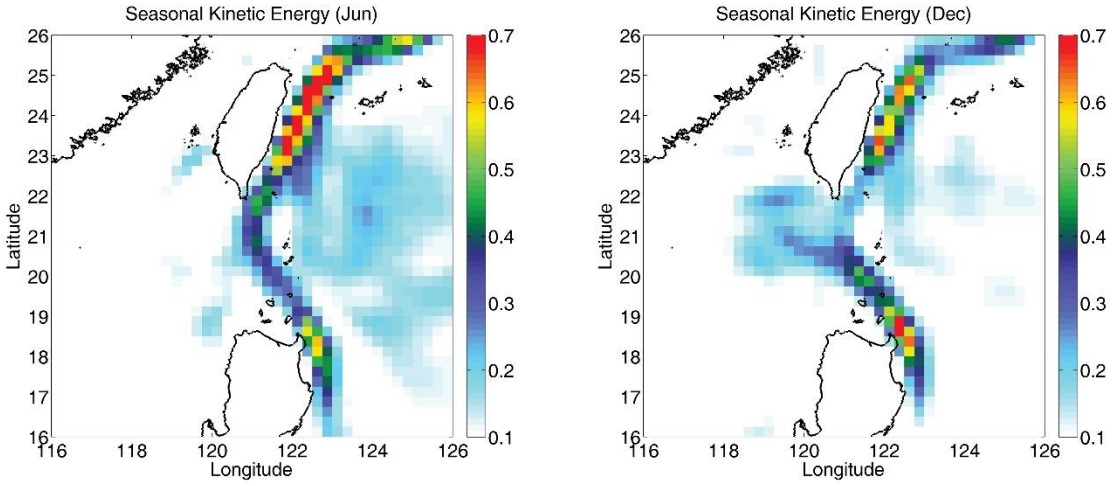

Figure 6: Seasonal kinetic energy in June (left) and December (right). Unit:m^2/s^2.

3.3 Dynamical mechanism from streamline analysis

3.3.1 Role of lateral velocity shears

The streamline-based classification of the Kuroshio inflow regime is advantageous to distinguishing the characteristics of different streamline types, and thus provides some new insights into the intrusion mechanisms. Figure 7 demonstrates the bin-averaged vorticity of the Leak and Leap streamlines in June and December respectively. It is very conspicuous that the majority of the Leak streamlines have positive vorticity while most Leap streamlines keep negative vorticity on the way north. The negative magnitudes of the Leap streamlines are about the same between seasons, in line with the transport variation (Fig.6). In winter, the strong intrusion can bring the positive vorticity into the SCS. The clear separation between different streamlines and vorticity polarity is obviously linked with the horizontal velocity shears. The outer half part of the Kuroshio streamlines, accounting for about 55% of the total in winter (deduced from Table 1), always leap across the LS under the influence of their anticyclonic velocity shear, whether it is in summer or winter. That is to say, the seasonal variation of the Kuroshio intrusion is merely the variation of the inner part of the flow, i.e., the part with cyclonic velocity shear. The pattern of the loop case looks more or less like that of the leap in winter (not shown). In summer the Loop streamlines are too few to draw statistically significant

conclusions like the Leak ones.

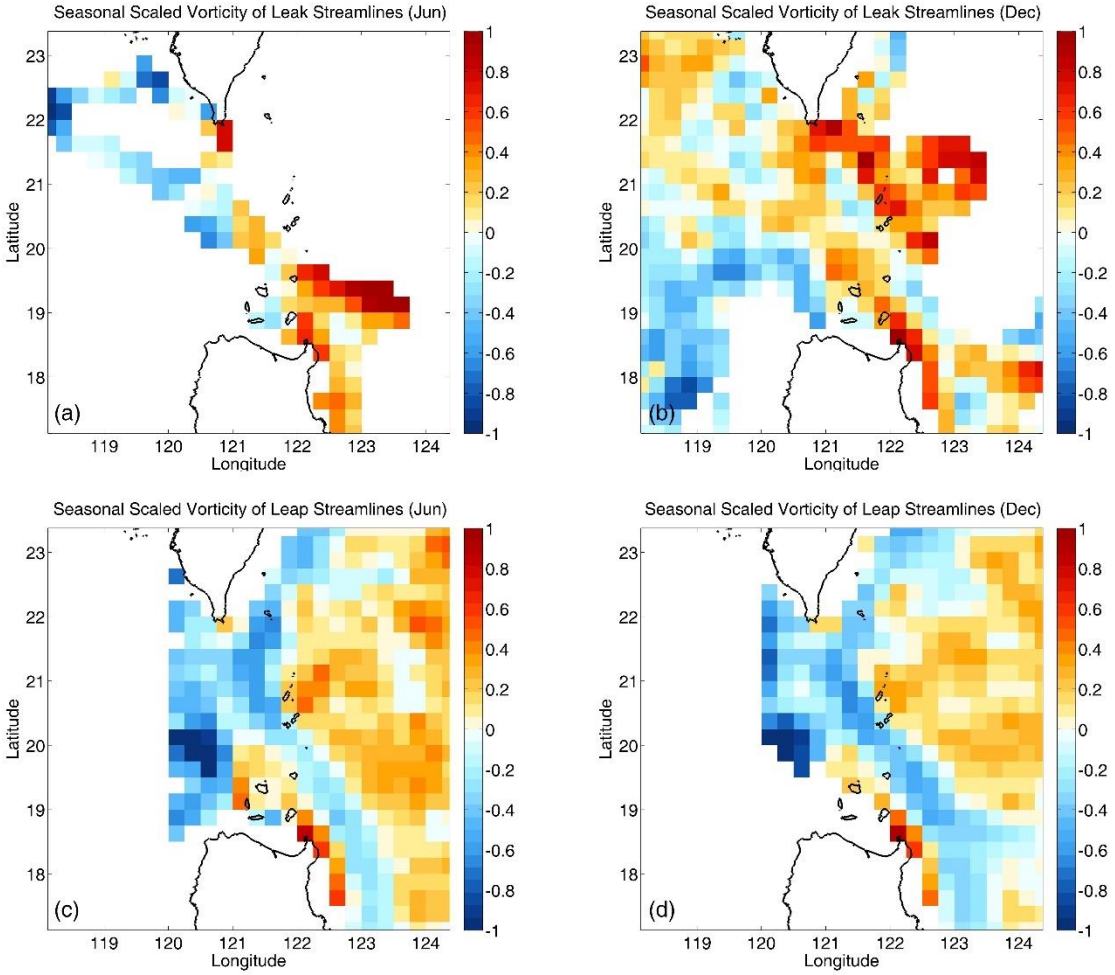

Figure 7: Seasonal relative vorticity of Leak and Leap streamlines in June and December. The vorticity is nondimensionalized by *f*.

The kinetic energy reduces to some degree along the streamlines, as the streamlines spread out after the jet inflow loses contact with the wall boundary (Fig.8). It is interesting to note that the kinetic energy is not divided half-and-half in December when the current bifurcates in the LS (Fig. 8b, d). Less energy is carried with the Leap streamlines, even they account for 55% of the total. This uneven energy distribution implies a larger portion of kinetic energy possessed by the positive vorticity part of the current in winter. In summer the Leap streamlines have a higher energy level for very few intrusions occur during this season.

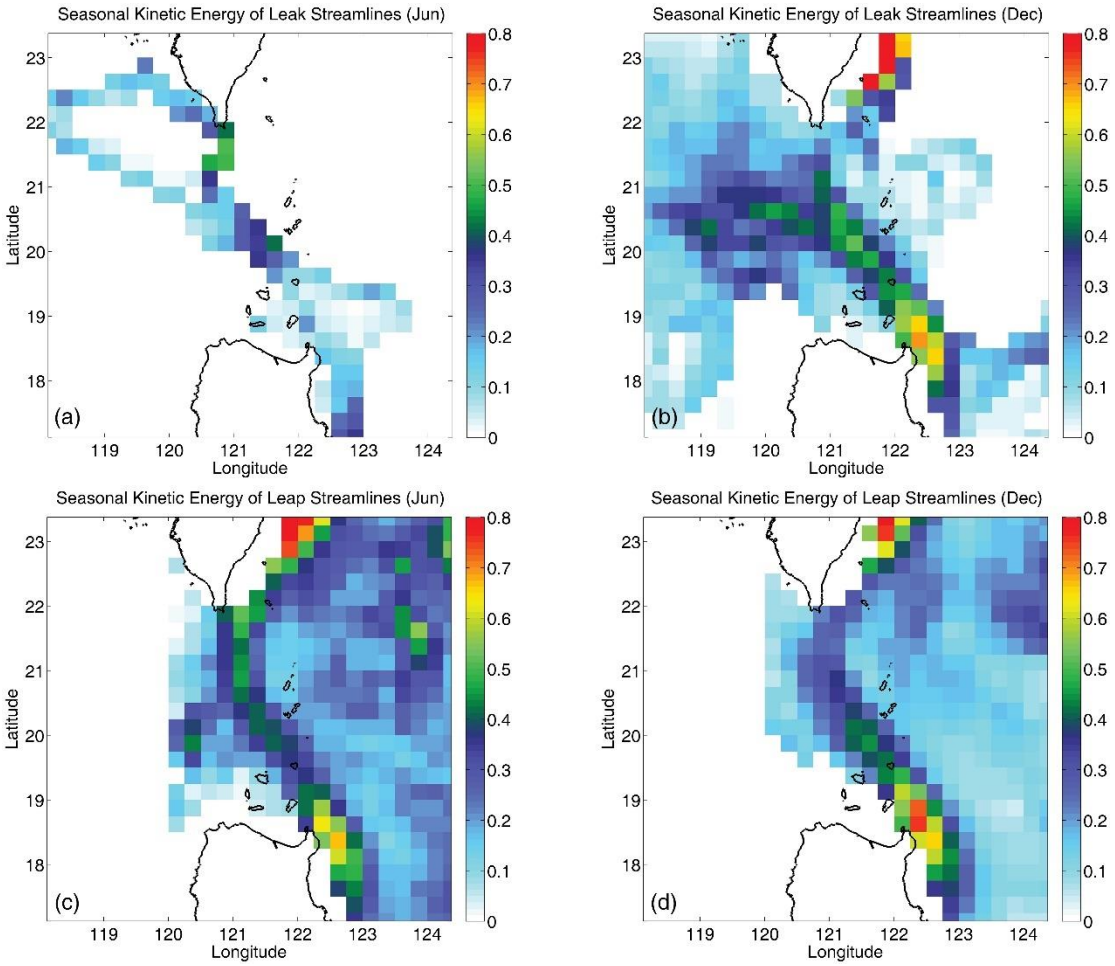

348

349 Figure 8: Seasonal kinetic energy of Leak and Leap streamlines. (Unit: m^2/s^2)

350 ### 3.3.2 Influences of seasonal monsoon

351 Given the geostrophic streamlines used in this study, the effect of direct Ekman
352 transport is naturally ruled out. Nevertheless, winds can still be at play by lifting or
353 depressing the sea surface level near the lateral boundary or by the stress curl as a
354 vorticity forcing. By a quick check of historical hydrographic profiles, the
355 deformation radius is approximately 10 km, limited to a narrow strip along the coast.
356 However, the current axis in all seasons is close enough to the coast so that a
357 considerable portion of the cyclonic shear part of the upstream current shall be largely
358 influenced by the wind. Owing to the coarse resolution of the altimeter data, the
359 numerical computation of the velocity difference is not accurate enough, so only
360 qualitative conclusions about this effect may be inferred here. The northeasterly

monsoon in winter would pile up the water near the coast, which may reduce the Kuroshio intensity by flattening the surface slope and/or even induce a southward longshore current. Either of them or their combination can increase the cyclonic velocity shear within the boundary layer of the current. The opposite occurs in summer with a weakened lateral velocity shear. This speculation seems reasonable because the seasonal variation of positive vorticity fluxes into the western boundary layer associated with the cyclonic shears have to balance the seasonality of the basin-wide negative wind stress curl, according to the classical wind-driven circulation theory. In addition, given the position, intensity and surface transport of the Kuroshio show little seasonality, this process is practically left to be the only candidate to balance the seasonal wind stress curl input.

The seasonal wind stress curls over the intrusion region are shown in Figure 9. The wind product is obtained from QuikSCAT-NCEP blended dataset (Milliff et al., 2004; Northwest Research Associates/Inc., 2001). The scatterometer measures the winds relative to the current, which seems more reliable in the strong current region (Plagge et al., 2012). A notable feature in winter is that extremely large stress curls only occur southwest of Taiwan and northeast of Philippine, while the magnitude in the Pacific sector is nearly an order smaller, very much like that in summer (Fig.9). Over the upstream Kuroshio region ahead of intrusion, the mean vorticity change rate calculated from satellite data is typically of the order of 10^{-9}~$10^{-7}s^{-2}$ depending on the season. The vorticity contribution from the wind is estimated to be $10^{-10}s^{-2}$ even for the strong curl regions. Such a weak stress curl is thus expected to have a negligible impact on the mixed layer vorticity budget, in agreement with the vorticity analysis results from Nan et al. (2011a). Wu and Hsin (2012) presents the negative curl off southwest Taiwan is strongly correlated with the depth-averaged kinetic energy in the center of Luzon Strait, suggesting that the wind curl can help the Kuroshio intrusion into the SCS. In this study with the surface streamlines we only attempt to investigate the link between the intensity of this curl and the surface intrusion probability, i.e., the total percentage of the Leak and Loop streamlines. The correlation between them

turns out to be very weak (below 0.4). Since the satellite data limit our analysis to the surface only, no further exploration can be done on how this discrepancy comes about.

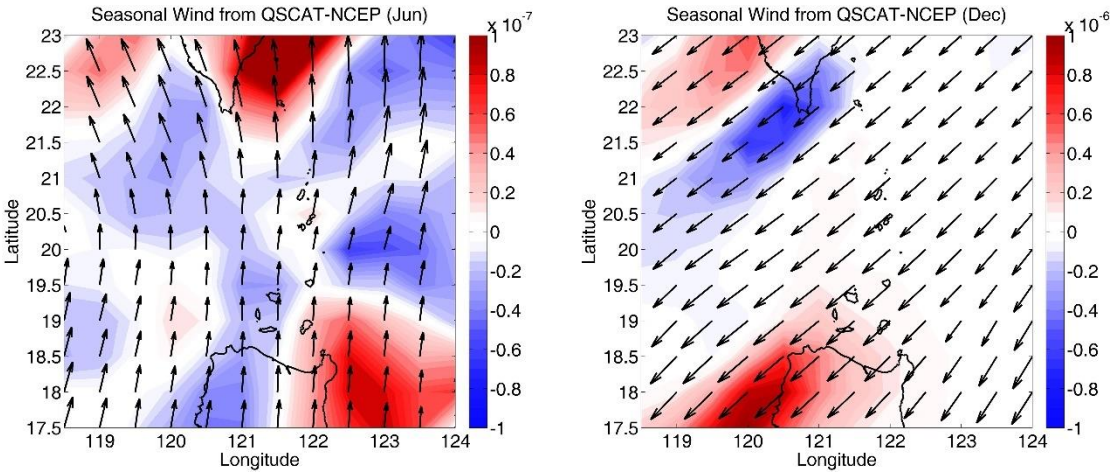

Figure 9: Seasonal wind vectors and wind stress curls (shaded, Unit: N/m^3) derived from QSCAT-NCEP blended wind in June (left) and December (right). Note that the magnitude is an order difference between the two panels.

3.3.3 A possible mechanism for Kuroshio intrusion

In light of the weak seasonality of the Kuroshio intensity, position and width, the strong seasonal cycle of the geostrophic Kuroshio intrusion poses a question in explaining the controlling mechanism behind, which the theories reviewed in Section 1 cannot well address. In this section we attempt to seek a suitable interpretation to accommodate all the seasonal characteristics of Kuroshio intrusion discussed above. In particular, the divergence of streamlines with positive and negative vorticities shed some light on what determines the current to leap across or leak into the Strait. However, the data resolution is so coarse that the western boundary current is covered by only a few grid points (Fig.6). Any numerical computation on high-order derivatives could cause unanticipated errors in such a dynamic region. As a consequence, we will have to conjecture the mechanism of Kuroshio intrusion to a certain extent based on classical theories. We shall consider this issue from a “global”

410 and a “local” perspective (Figure 10).

411 From a “global” view, the basin-wide negative wind curls drive an anticyclonic
412 circulation with negative vorticity (anticyclonic velocity shear). In other words, the
413 anticyclonic velocity shear of the current reflects the anticyclonic flow tendency in
414 response to the negative wind curl forcing. A counteracting effect is required to brake
415 the current and maintain the vorticity balance or the torque balance with the wind
416 forces. This work can be done by the lateral friction force according to Munk’s theory
417 (Munk, 1950), which dissipates the flow energy and induces cyclonic shears of the
418 boundary current by imposing a positive torque. The anticyclonic shear part of the
419 flow always has a tendency to lead the current northward to close up the anticyclonic
420 gyre, whether there is a gap on the western boundary or not. Stated from the vorticity
421 perspective, the positive vorticity fluxes into the western boundary flow at each
422 latitude are exactly in balance with the negative vorticity inputs by wind stress
423 (Pedlosky, 2010). Once the flow encounters a boundary gap, the positive vorticity
424 source is shut down and the unbalanced negative vorticity associated with the
425 anticyclonic velocity shear would drive the current northward to a place with higher
426 ambient vorticity.

427 The “local” view zooms into the western boundary region, where the cyclonic
428 friction torque imposed by the wall must be locally balanced to keep the flow steady.
429 The local wind stress curls have been seen to be too weak to counteract this torque
430 (Fig.9). As a matter of fact, it is the torque of the normal stresses exerted by the wall
431 boundary that provide such a counteracting effect. An analog in rigid body dynamics
432 is that if a solid cube is pushed forwards on a frictional surface, the torque of friction
433 forces must be balanced by the torque of normal forces to prevent the cube from
434 rolling over. In the fluid case here, the non-uniform normal stresses generate a
435 negative torque against the friction stresses to keep the current parallel to the
436 boundary (red and green arrows in Fig. 10). It is worthwhile to clarify the difference
437 from the wind-friction torque balance discussed in the “global” view. The torque of

normal stresses doesn't do any work because no displacement perpendicular to the boundary is allowed. For this reason, the aforementioned wind-friction torque balance should be stated more exactly as the balance between the work done by the wind stress torque and by the friction stress torque along the western boundary. The vorticity is produced by the torque work, so the vorticity balance should involve only the wind and the friction effects. When the boundary current encounters a gap, it immediately loses the normal stress torque and is bent into the gap by the positive torque of interior shear stresses left by the lateral friction. The interior shear stress is usually parameterized in the form of $A_H \partial^2 v/\partial x^2$. A very loose calculation using satellite data shows it is indeed positive for the entire current in line with Munk's solution. This explains why most of Kuroshio streamlines always meander through the LS (Fig. 2). It is also the hydrodynamic interpretation of the "teapot effect" (Kistler & Scriven, 1994).

Based on the "global" and "local" viewpoints, we see that there is a competition in the Kuroshio Current between a cyclonic tendency of movement due to the local unbalanced positive torque of interior shear stresses and an anticyclonic tendency of movement due to the global negative vorticity forcing of wind stresses. The kinematic structures of the Kuroshio are very similar over all seasons except a coastal strip where the cyclonic velocity shear might be significantly modified by the seasonally-reversing monsoon. Therefore, the Leap streamlines, located mostly on the outer part of the flow, are always prone to flow anticyclonically following a stable path regardless of seasons (Fig.3 and 4). In contrast, the inner part of the flow is largely influenced by the seasonally-varying cyclonic velocity shears. In summer, the monsoon-induced longshore current may weaken the interior stress torque, which is then not able to resist the anticyclonic tendency, therefore the entire current leaps across the Strait. On the contrary, the cyclonic interior stress torque is strengthened by the monsoon in winter so that this portion of the streamlines is torn apart from the main stream and intrude westwards into the SCS.

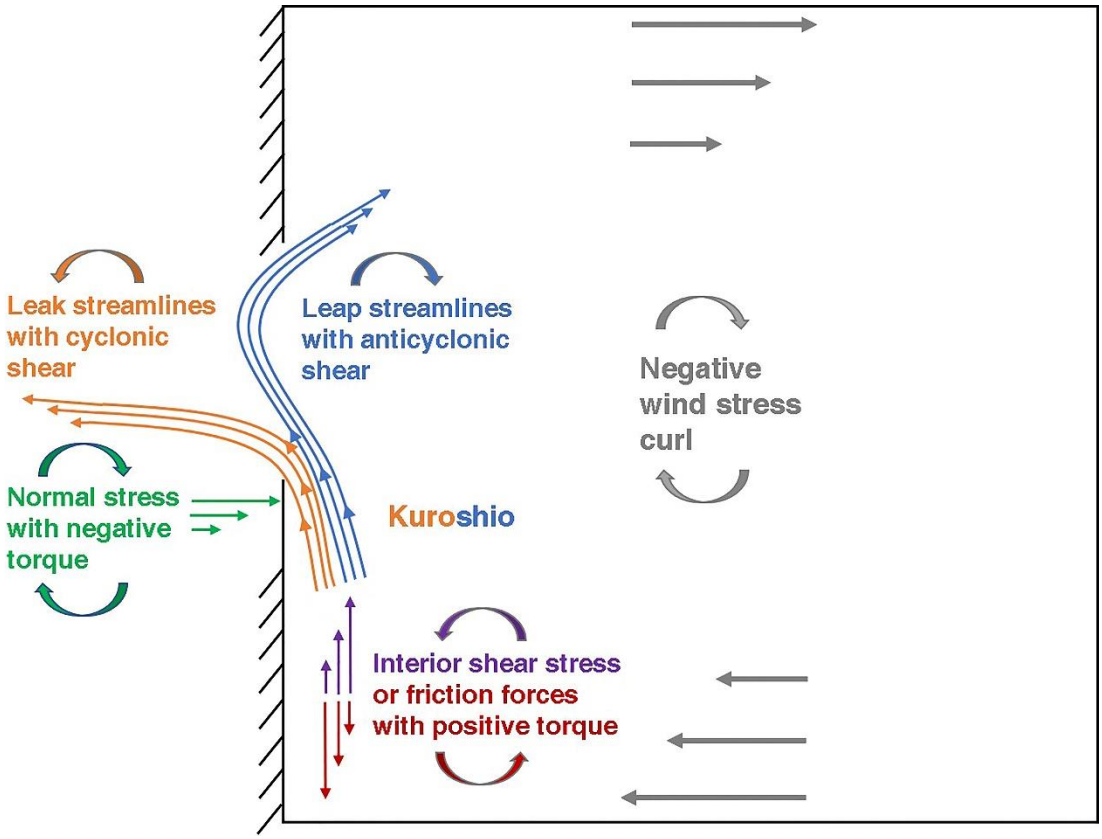

466

467 Figure 10: Sketch of the ‘global’ and ‘local’ views of Kuroshio intrusion

468 **4. Discussion and conclusions**

469 We have developed a streamline-based algorithm to identify the intrusion types
470 and make a thorough investigation on the seasonality of a number of Kuroshio
471 intrusion properties using satellite altimeter data. Unlike the results from previous
472 identification methods, it turns out that a mixed type with all kinds of streamlines is
473 the dominant flow pattern in winter. The streamline entrance locations into the LS
474 vary depending only on the streamline types, and the intensity, width and current axis
475 of the Kuroshio also show insignificant seasonal variabilities. The use of geostrophic
476 velocities precludes the direct Ekman transport effect, and the magnitude of local
477 wind stress curls is too small to influence the upstream Kuroshio into the LS.

478 In light of all these characteristics, it appears that none of the physical
479 mechanisms proposed by preceding studies could fully explain the seasonal intrusion
480 variability. Noting a clear partition between the Leak streamlines with cyclonic

velocity shears and the Leap streamlines with anticyclonic shears, we present a new interpretation based on globally the vorticity balance (torque work balance) between negative wind curl input and positive frictionally-induced vorticity fluxes, and locally the loss of balance between the interior stress torque and the normal stress torque both provided by the wall boundary. Due to the coarse resolution of satellite data, a conjecture has to be made that the seasonally-reversing monsoon would significantly modify the cyclonic velocity shears in the inner part of the Kuroshio, leading to the seasonal variations of the interior stress torque and thus the Kuroshio intrusion. Given that the basin-wide wind curl is also seasonally-varying, which must be balanced by frictionally-induced vorticity, we anticipate that this conjecture should be reasonable.

The physical interpretation we discussed above attributes the seasonal variation of Kuroshio intrusion to a single external factor — the local monsoon and a series of dynamical processes. It doesn't mean that other factors have no influence on the intrusion, but that the monsoon merely stands out under some certain kinetic conditions of Kuroshio on the seasonal scale. For example, we also anticipate that the current inertia characterized by Reynolds number $Re = Q/A_H$ is an important factor (Sheremet 2001), though the Kuroshio transport Q is roughly invariant on the seasonal scale. On an interannual scale, the shift of the north equatorial current bifurcation may change the Kuroshio transport and further affect the Kuroshio intrusion (e.g. Kim et al., 2004). Sheremet (2001) also shows the occurrence of hysteresis in the flow evolution, which is considered to be averaged out over a seasonal time scale. The direct Ekman effect by the monsoon could be also important to enhance the intrusion in the LS (Wu & Hsin, 2012), but our method is unable to evaluate its contribution.

One possible issue with satellite-derived streamlines is that the geostrophic current may not well represent the true current, especially within the boundary layer where the lateral friction is a significant term in the momentum balance. In addition, the lateral friction could also be important to the wind setup of surface elevations near

the coast. High-resolution nearshore in-situ measurements or numerical simulations with a proper parameterization are needed to examine the role of the lateral friction and corroborate the theory discussed above. One may also argue that the streamlines are in Eulerian but not Lagrangian framework. The typical magnitude of absolute dynamical height is 1 m while its daily variation is of the order of 10^{-2}m over the intrusion region. With the intrusion path of 300 km and the current speed of 0.6m/s, we get a time scale of about 6 days. So, it should be safe to assume the flow is approximately stationary over a full period of Kuroshio intrusion.

5. Acknowledgements

The altimeter data provided by E. U. Copernicus Marine Service Information is downloaded from http://marine.copernicus.eu/services-portfolio/access-to-products/?option=com_csw&view=details&product_id=SEALEVEL_GLO_PHY_CLIMATE_L4_REP_OBSERVATIONS_008_057. The QSCAT-NCEP blended dataset is obtained from https://rda.ucar.edu/datasets/ds744.4. The data products are properly cited and referred in the reference list. This work is supported by the grants from the National Natural Science Foundation of China (No. 41706014), the Sino-German Cooperation in ocean and polar research – Megacity's fingerprint in Chinese marginal seas: Pollutant fingerprints and dispersal transformation (MEGAPOL), the International Cooperation of the National Natural Science Foundation of China (No. 41861134040) and the National Program on Key Basic Research Project of China (973 Program, No. 2014CB441500). J.W. is supported by MEGAPOL with the contract number to it BMBf (03F0786A) Federal Ministry of Education and Research and SOCLIS-SO269 FKZ 03G0269. L.Z. is supported by the National Natural Science Foundation of China (No. 41690121, 41690120, 41530961)

References

Caruso, M. J., Gawwarkiewicz, G. G. & Beardsley, R. C. (2006). Interannual variability of the Kuroshio intrusion in the South China Sea. *Journal of Oceanography*, *62*, 559–575.

https://doi.org/ 10.1007/s10872-006-0076-0.

Chang, Y.-L. & Oey, L.-Y. (2011). Interannual and seasonal variations of Kuroshio transport east of Taiwan inferred from 29 years of tide-gauge data. *Geophysical Research Letters, 38*, L08603. https://doi.org/10.1029/2011GL047062.

Chen, Y., Zhai, F. & Li, P. (2020). Decadal variation of the Kuroshio intrusion into the South China Sea During 1992-2016. *Journal of Geophysical Research, 125*, e2019JC015699. https://doi.org/10.1029/2019JC015699.

Farris, A. & Wimbush, M. (1996). Wind-induced Kuroshio intrusion into the South China Sea. *Journal of Oceanography, 52*, 771–784. https://doi.org/10.1007/BF02239465.

Hsin, Y.-C., Wu, C.-R. & Chao, S.-Y. (2012). An updated examination of the Luzon Strait transport. *Journal of Geophysical Research, 117*, C03022. https://doi.org/10.1029/2011JC007714.

Kim, Y.Y., Qu, T., Jensen, T., Miyama, T., Mitsudera, H., Kang, H.-W. & Ishida, A. (2004). Seasonal and interannual variations of the North Equatorial Current bifurcation in a high-resolution OGCM. *Journal of Geophysical Research, 109*, C03040. https://doi.org/10.1029/2003JC002013.

Kistler, S. F. & Scriven, L. E. (1994). The teapot effect: Sheet-forming flows with deflection, wetting and hysteresis. *Journal of Fluid Mechanics, 263***,** 19–62. https://doi.org/10.1017/S0022112094004027.

Kuehl, J. J. & Sheremet, V. A. (2009). Identification of a cusp catastrophe in a gap-leaping western boundary current. *Journal of Marine Research, 67*, 25–42. https://doi.org/10.1357/002224009788597908

Lan, J., Bao, X. & Gao, G. (2004). Optimal estimation of zonal velocity and transport through Luzon Strait using variational data assimilation technique. *Chinese Journal of Oceanology and Limnology, 22*, 335–339. https://doi.org/10.1007/BF02843626.

Liang, W.-D., Tang, T. Y., Yang, Y. J., Ko, M. T. & Chuang, W.-S. (2003). Upper-ocean currents around Taiwan. *Deep-Sea Research II: Topical Studies in Oceanography, 50*, 1085–1105. https://doi.org/10.1016/S0967-0645(03)00011-0.

Liang, W.-D., Yang, Y.J., Tang, T.Y. & Chuang, W.-S. (2008). Kuroshio in the Luzon Strait. *Journal of Geophysical Research, 113*, C08048. https://doi.org/10.1029/2007JC004609.

Metzger, E. J. & Hurlburt, H. E. (1996). Coupled dynamics of the South China Sea, the Sulu Sea, and the Pacific Ocean. *Journal of Geophysical Research, 101*(C5), 12 331–12352. https://doi.org/10.1029/95JC03861.

Metzger, E. J. & Hurlburt, H. E. (2001). The nondeterministic nature of Kuroshio penetration and

eddy shedding in the South China Sea. *Journal of Physical Oceanography, 31*(7), 1712–1732. https://doi.org/ 10.1175/1520-0485(2001)031<1712:TNNOKP>2.0.CO;2.

Milliff, R. F., Morzel., J., Chelton, D. B. & Freilich, M. H. (2004). Wind stress curl and wind stress divergence biases from rain effects on QSCAT surface wind retrievals. *Journal of Atmospheric and Oceanic Technology, 21*(8), 1216–1231. https://doi.org/10.1175/1520-0426(2004)021<1216:WSCAWS>2.0.CO;2.

Munk, W. H. (1950). On the wind-driven ocean circulation. *Journal of Meteorology, 7*(2),79–93. https://doi.org/10.1175/1520-0469(1950)007<0080:OTWDOC>2.0.CO;2.

Nan, F., Xue, H., Chai, F., Shi, L., Shi, M. & Guo, P. (2011a). Identification of different types of Kuroshio intrusion into the South China Sea. *Ocean Dynamics, 61*, 1291–1304. https://doi.org/10.1007/s10236-011-0426-3.

Nan, F., Xue, H., Xiu, P., Chai, F., Shi, M. & Guo, P. (2011b). Oceanic eddy formation and propagation southwest of Taiwan. *Journal of Geophysical Research, 116*, C12045. https://doi.org/10.1029/2011JC007386.

Northwest Research Associates/Inc. (2001), QSCAT/NCEP Blended Ocean Winds from Colorado Research Associates (version 5.0), https://doi.org/10.5065/XQYC-1602, Research Data Archive at the National Center for Atmospheric Research, Computational and Information Systems Laboratory, Boulder, Colo. Accessed 9 Apr 2020.

Pedlosky, J. (2010). Ocean Circulation Theory. Springer Berlin Heidelberg

Plagge, A. M., Vandemark, D. & Chapron, B. (2012). Examining the impact of surface currents on satellite scatterometer and altimeter ocean winds. *Journal of Atmospheric and Oceanic Technology, 29*(12), 1776–1793. https://doi.org/10.1175/JTECH-D-12-00017.1.

Qu, T. (2000). Upper-layer circulation in the South China Sea. *Journal of Physical Oceanography, 30*(6), 1450–1460. https://doi.org/10.1175/1520-0485(2000)030<1450:ULCITS>2.0.CO;2.

Qu, T., Kim, Y. Y., Yaremchuk, M., Tozuka, T., Ishida, A. & Yamagata, T. (2004). Can Luzon strait transport play a role in conveying the impact of ENSO to the South China Sea? *Journal of Climate, 17*(18), 3644–3657. https://doi.org/10.1175/1520-0442(2004) 017<3644:CLSTPA>2.0.CO;2.

Sheremet, V. A. (2001). Hysteresis of a western boundary current leaping across a gap. *Journal of Physical Oceanography, 31*(5), 1247–1259. https://doi.org/10.1175/1520-0485(2001)031<1247:HOAWBC>2.0.CO;2

Sheu, W.-J., Wu, C.-R. & Oey, L.-Y. (2010). Blocking and westward passage of eddies in the Luzon Strait. *Deep-Sea Research II: Topical Studies in Oceanography, 57*, 1783–1791. https://doi.org/10.1016/j.dsr2.2010.04.004.

Song, Y. T. (2006). Estimation of interbasin transport using ocean bottom pressure: theory and model for Asian marginal seas. *Journal of Geophysical Research, 111*, C11S19. https://doi.org/10.1029/2005JC003189.

Wu, C.-R. (2013). Interannual modulation of the Pacific Decadal Oscillation (PDO) on the low-latitude western North Pacific. *Progress in Oceanography, 110*, 49–58. https://doi.org/10.1016/j.pocean.2012.12.001.

Wu, C.-R. & Hsin, Y.-C. (2012). The forcing mechanism leading to the Kuroshio intrusion into the South China Sea. *Journal of Geophysical Research, 117*, C07015. https://doi.org/10.1029/2012JC007968.

Xu, J. P., Shi, M. C., Zhu, B. K. & Liu, Z. H. (2004). Several characteristics of water exchange in the Luzon Strait. *Acta Oceanologica Sinica, 23* (1), 11–22.

Xu, J. P. & Su, J. L. (2000). Hydrological analysis of Kuroshio water intrusion into the South China Sea. *Acta Oceanologica Sinica, 19* (3), 1–21.

Xue, H. J., Chai, F., Pettigrew, N. R., Xu, D. Y., Shi, M. C. & Xu, J. P. (2004). Kuroshio intrusion and the circulation in the South China Sea. *Journal of Geophysical Research, 109*, C02017. https://doi.org/10.1029/2002JC001724.

Yang, Q., Tian, J. & Zhao, W. (2010). Observation of Luzon Strait transport in summer 2007. *Deep-Sea Research I: Oceanographic Research Papers, 57*(5), 670–676. https://doi.org/10.1016/j.dsr.2010.02.004.

Yang, J., Lin, X. & Wu, D. (2013). On the dynamics of the seasonal variation in the South China Sea throughflow transport. *Journal of Geophysical Research Oceans, 118*(12), 6854–6866. https://doi.org/10.1002/2013JC009367.

Yaremchuk, M. & Qu, T. (2004). Seasonal variability of the large-scale currents near the coast of the Philippines. *Journal of Physical Oceanography, 34*(4), 844–855. https://doi.org/ 10.1175/1520-0485(2004)034<0844:SVOTLC>2.0.CO;2.

Yuan, Y., Liao, G., Guan, W., Wang, H., Lou, R. & Chen, H. (2008). The circulation in the upper and middle layers of the Luzon Strait during spring 2002. *Journal of Geophysical Research, 113*, C06004. https://doi.org/10.1029/2007JC004546.

Yuan, D. L., Han, W. Q. & Hu, D. X. (2006). Surface Kuroshio path in the Luzon Strait area derived from satellite remote sensing data. *Journal of Geophysical Research, 111*, C11007. https://doi.org/10.1029/2005JC003412.